X Hotine-Marussi Symposium 2022

Coestimating long-term temporal signals to reduce the aliasing effect in parametric geodetic mean dynamic topography estimation

Jan Martin Brockmann[1], Moritz Borlinghaus[1], Christian Neyers[1] and Wolf-Dieter Schuh[1]

[1] Institute of Geodesy and Geoinformation · Theoretical Geodesy Group · University of Bonn

June 16, 2022

Overview: Parametric Geodetic MDT Estimation

Along track altimetric SSH observations

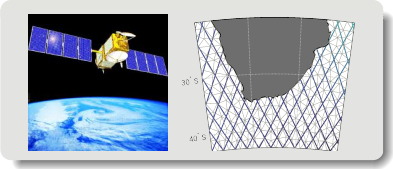

Overview: Parametric Geodetic MDT Estimation

Along track altimetric SSH observations

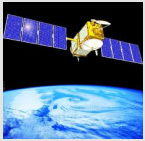

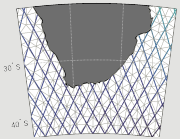

signal separation & spatial and temporal averaging

geoid: parameterized as global spherical harmonics
range ± 100 m

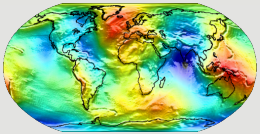

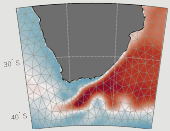

MDT: parameterized by local finite element basis functions
range ± 2 m

Overview: Parametric Geodetic MDT Estimation

Along track altimetric SSH observations

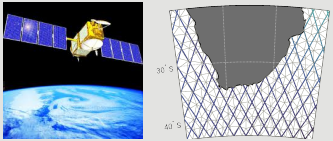

signal separation & spatial and temporal averaging

geoid: parameterized as global spherical harmonics
range ± 100 m

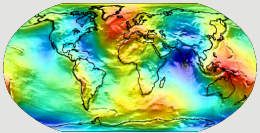

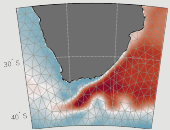

MDT: parameterized by local finite element basis functions
range ± 2 m

- satellite-only, e.g. GOCO
- band-limited in spherical harmonic domain
- stochastic data

gravity field data

Overview: Parametric Geodetic MDT Estimation

Along track altimetric SSH observations

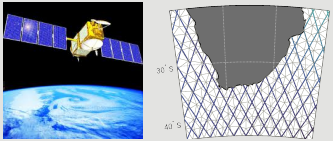

signal separation & spatial and temporal averaging

geoid: parameterized as global spherical harmonics
range ±100 m

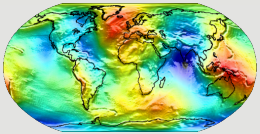

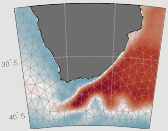

MDT: parameterized by local finite element basis functions
range ±2 m

- satellite-only, e.g. GOCO
- band-limited in spherical harmonic domain
- stochastic data

gravity field data

oceanographic data

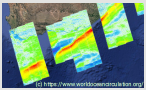

see poster: Neyers et al. today

Joint Estimation of MDT & Geoid

geoid/gravity

- observations: satellite-based gravity field NEQ (e.g. GOCO), smoothness
- full VCM + ommision
- spherical harmonics

$l_{GF}=f(x_{GF})$

sea surface height

- observations: along-track SSH of multiple missions (e.g. radar, **SWOT**)
- empirical error model
- potential: tide gauges

$l_{SSH}=f(x_{GF}, x_{DOT})$

oceanographic

observations: drifters, surface currents (e.g. SVP, SAR, SKIM), smoothness conditions

- empirical error model

$l_{OG}=f(x_{DOT})$

joint least squares adjustment

- Estimate gravity field & DOT
- seperation of SSH
- weighted combination
- high-dimensional, HPC
- spatial & temporal filtering

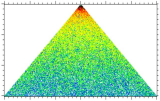

estimated parameters

refinened gravity field

- parametric model: spherical harmonics
- parameters: $x_{GF} = [\ c_{lm}, s_{lm}]$
- full VCM

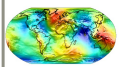

dynamic ocean topography

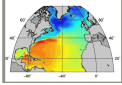

- parametric model: finite element space
- parameters: $x_{DOT} = [\ a_k(t)\ ]$
- Full VCM

DFG project PARASURV — PArametric determination of the dynamic ocean topography from geoid, altimetric sea surface heights and SAR derived RAdial SURface Velocities

details:
[8, 11, 2, 3, 10, 4, 9]

Finite Element Base Functions for Spatial Approximation

MDT represented as linear combination of finite element (FE) base functions $b_k(\theta, \lambda)$

$$\zeta(\theta, \lambda) = \sum_{k \in K} a_{\mathsf{MDT},k} b_{\mathsf{MDT},k}(\theta, \lambda), \qquad \mathbf{x}_{\mathsf{MDT}} = [a_{\mathsf{MDT},k}] \tag{1}$$

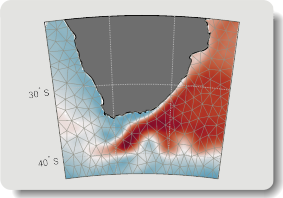

- continuous model in space (C^0/C^1-smooth)
- unknowns $a_{\mathsf{MDT},k}$ interpretable (e.g. DOT, derivatives, ...)
- FE space defines filtering/spatial resolution
- observation equations in any location and functional (point values, derivatives, integrals, ...)

Finite Element Base Functions for Spatial Approximation

MDT represented as linear combination of finite element (FE) base functions $b_k(\theta, \lambda)$

$$\zeta(\theta, \lambda) = \sum_{k \in K} a_{\mathsf{MDT},k} b_{\mathsf{MDT},k}(\theta, \lambda), \qquad \mathbf{x}_{\mathsf{MDT}} = [a_{\mathsf{MDT},k}] \tag{1}$$

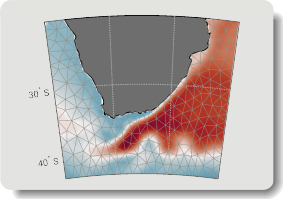

- continuous model in space (C^0/C^1-smooth)
- unknowns $a_{\mathsf{MDT},k}$ interpretable (e.g. DOT, derivatives, ...)
- FE space defines filtering/spatial resolution
- observation equations in any location and functional (point values, derivatives, integrals, ...)

C^0-smooth: linear element

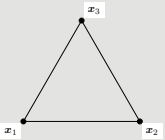

- 3 dof
- simple: DOT in nodes
- see [2, 3]

C^1-smooth: HCT element

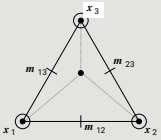

- 12 dof
- composed element
- see [5]

C^1-smooth: ARGYRIS element

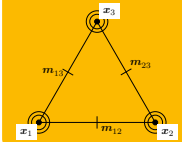

- 21 dof
- see [1, 9]

$\Rightarrow$ this study

Motivation: Altimetric SSH Sampling

ERM (e.g. Jason-1: repeat 10 d)

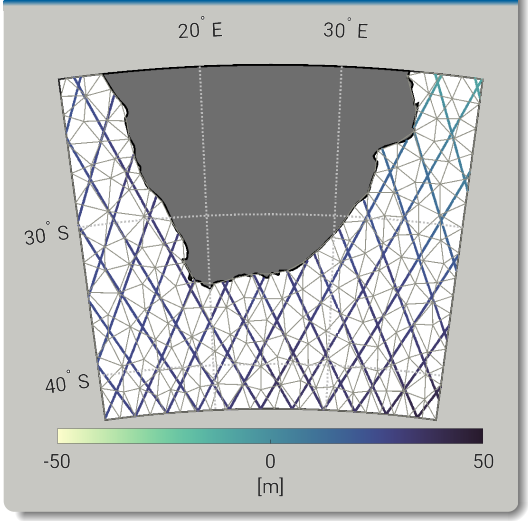

Motivation: Altimetric SSH Sampling

ERM (e.g. Jason-1: repeat 10 d)

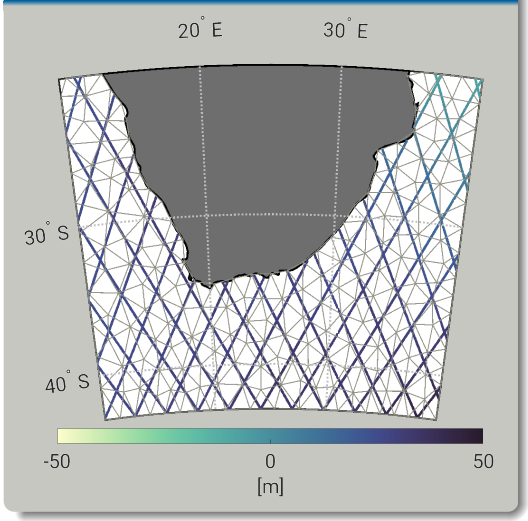

GM (e.g. Cryosat2: repeat 369 d)

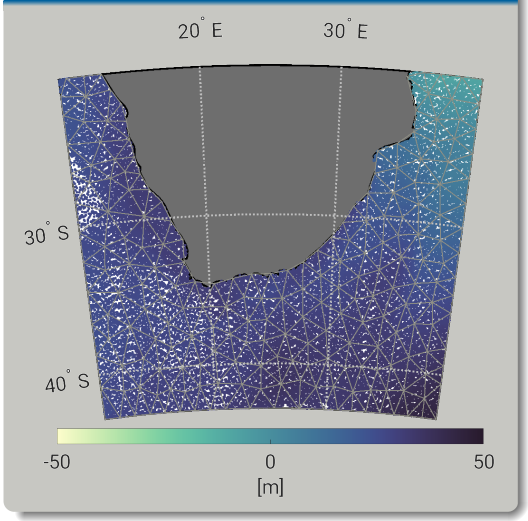

Motivation: Altimetric SSH Sampling

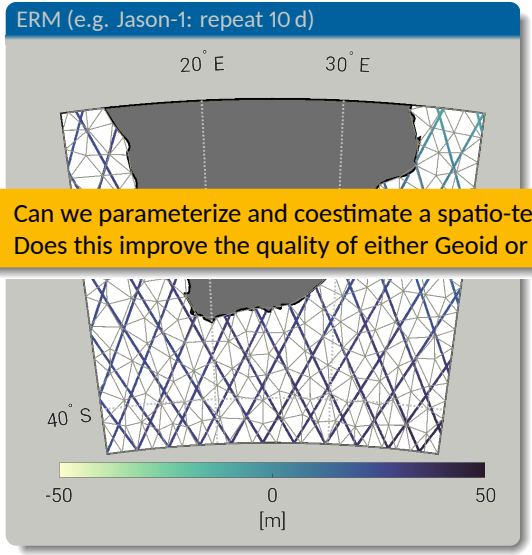

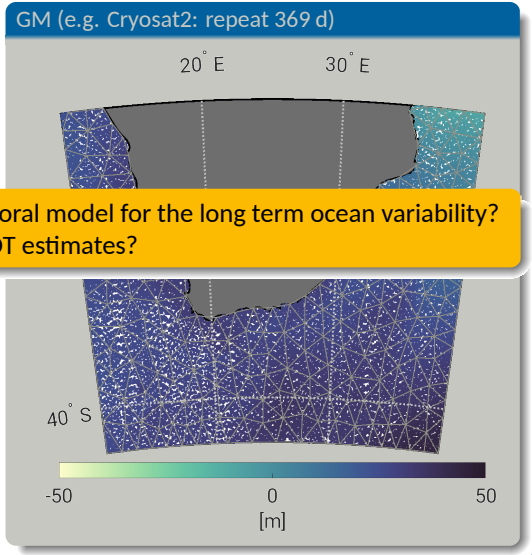

- Can we parameterize and coestimate a spatio-temporal model for the long term ocean variability?
- Does this improve the quality of either Geoid or MDT estimates?

Model A: Static SSH Observation Equations

Least-squares observation equations for altimetric SSH observations

$$l_i + v_i = N(\theta_i, \lambda_i) + \zeta(\theta_i, \lambda_i) \tag{2}$$

- $N(\theta_i, \lambda_i)$: geoid height, a function in the unknown spherical harmonic coefficients c_{lm} and s_{lm}
- $\zeta(\theta_i, \lambda_i)$: MDT, a function in the unknown FE scaling coefficients $a_{\text{MDT},k}$

Model A: Static SSH Observation Equations

Least-squares observation equations for altimetric SSH observations

$$l_i + v_i = N(\theta_i, \lambda_i) + \zeta(\theta_i, \lambda_i) \tag{2}$$

- $N(\theta_i, \lambda_i)$: geoid height, a function in the unknown spherical harmonic coefficients c_{lm} and s_{lm}
- $\zeta(\theta_i, \lambda_i)$: MDT, a function in the unknown FE scaling coefficients $a_{\text{MDT},k}$

$\Rightarrow$ Implicit temporal averaging by least squares: repeated measurements

Model A: Static SSH Observation Equations

Least-squares observation equations for altimetric SSH observations

$$l_i + v_i = N(\theta_i, \lambda_i) + \zeta(\theta_i, \lambda_i) \tag{2}$$

- $N(\theta_i, \lambda_i)$: geoid height, a function in the unknown spherical harmonic coefficients c_{lm} and s_{lm}
- $\zeta(\theta_i, \lambda_i)$: MDT, a function in the unknown FE scaling coefficients $a_{\text{MDT},k}$

$\Rightarrow$ Implicit temporal averaging by least squares: repeated measurements

Combined NEQs

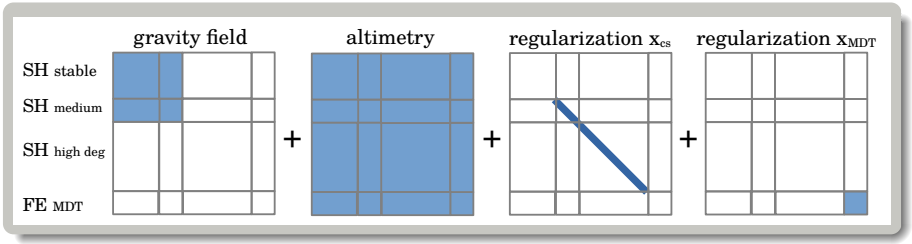

- Regularization: global high degree spherical harmonic coefficients to be solvable
- Regularization: to obtain a smooth MDT and to support separation $\Rightarrow \min \|\nabla\zeta(\theta, \lambda)\|$

Model B: Temporal SSH Observation Equations

Least-squares observation equations for altimetric SSH observations

$$l_i + v_i = N(\theta_i, \lambda_i) + \zeta(\theta_i, \lambda_i) + OV(\theta_i, \lambda_i, t_i) \tag{3}$$

Coestimating a separable spatial (FE as for ζ) & temporal model to compensate the ocean variability

$$OV(\theta_i, \lambda_i, t_i) = \sum_{l \in L} a_{\mathrm{ov},l}(t) b_{\mathrm{ov},l}(\theta, \lambda) = \sum_{l \in L} \sum_{k \in K} e_{\mathrm{ov},k,l} h_{\mathrm{ov},k}(t) b_{\mathrm{ov},l}(\theta, \lambda) \tag{4}$$

Model B: Temporal SSH Observation Equations

Least-squares observation equations for altimetric SSH observations

$$l_i + v_i = N(\theta_i, \lambda_i) + \zeta(\theta_i, \lambda_i) + OV(\theta_i, \lambda_i, t_i) \tag{3}$$

Coestimating a separable spatial (FE as for ζ) & temporal model to compensate the ocean variability

$$OV(\theta_i, \lambda_i, t_i) = \sum_{l \in L} a_{\mathrm{ov},l}(t) b_{\mathrm{ov},l}(\theta, \lambda) = \sum_{l \in L} \sum_{k \in K} e_{\mathrm{ov},k,l} h_{\mathrm{ov},k}(t) b_{\mathrm{ov},l}(\theta, \lambda) \tag{4}$$

With separable function to model a linear trend and a seasonal period

$$a_{\mathrm{ov},l}(t_i) = e_{\mathrm{ov},1,l} t_i + e_{\mathrm{ov},2,l} \sin(\omega t_i) + e_{\mathrm{ov},3,l} \cos(\omega t_i) \tag{5}$$

Model B: Temporal SSH Observation Equations

Least-squares observation equations for altimetric SSH observations

$$l_i + v_i = N(\theta_i, \lambda_i) + \zeta(\theta_i, \lambda_i) + OV(\theta_i, \lambda_i, t_i) \tag{3}$$

Coestimating a separable spatial (FE as for ζ) & temporal model to compensate the ocean variability

$$OV(\theta_i, \lambda_i, t_i) = \sum_{l \in L} a_{\mathrm{ov},l}(t) b_{\mathrm{ov},l}(\theta, \lambda) = \sum_{l \in L} \sum_{k \in K} e_{\mathrm{ov},k,l} h_{\mathrm{ov},k}(t) b_{\mathrm{ov},l}(\theta, \lambda) \tag{4}$$

With separable function to model a linear trend and a seasonal period

$$a_{\mathrm{ov},l}(t_i) = e_{\mathrm{ov},1,l} t_i + e_{\mathrm{ov},2,l} \sin(\omega t_i) + e_{\mathrm{ov},3,l} \cos(\omega t_i) \tag{5}$$

Model B: Temporal SSH Observation Equations

Least-squares observation equations for altimetric SSH observations

$$l_i + v_i = N(\theta_i, \lambda_i) + \zeta(\theta_i, \lambda_i) + OV(\theta_i, \lambda_i, t_i) \tag{3}$$

Coestimating a separable spatial (FE as for ζ) & temporal model to compensate the ocean variability

$$OV(\theta_i, \lambda_i, t_i) = \sum_{l \in L} a_{\mathrm{OV},l}(t) b_{\mathrm{OV},l}(\theta, \lambda) = \sum_{l \in L} \sum_{k \in K} e_{\mathrm{OV},k,l} h_{\mathrm{OV},k}(t) b_{\mathrm{OV},l}(\theta, \lambda) \tag{4}$$

With separable function to model a linear trend and a seasonal period

$$a_{\mathrm{OV},l}(t_i) = e_{\mathrm{OV},1,l} t_i + e_{\mathrm{OV},2,l} \sin(\omega t_i) + e_{\mathrm{OV},3,l} \cos(\omega t_i) \tag{5}$$

Combined NEQs

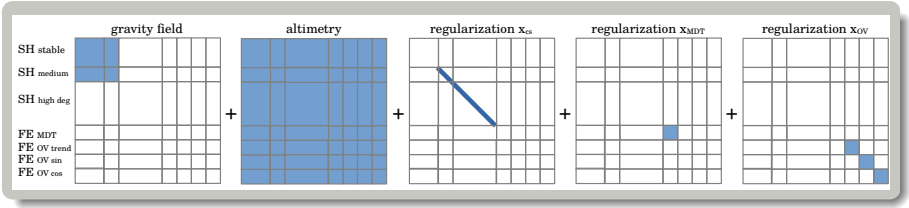

Configuration of Numerical Experiment

Study region

200 km mesh created by JIGSAW [6]

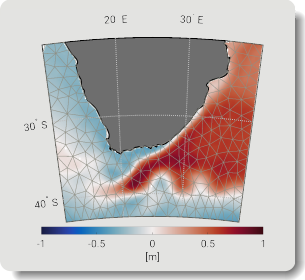

Gravity field information

- satellite-only model
- unconstrained GOCO06S normal equations
- spherical harmonic degree 2 to 300
- further details: [7]

Along track SSH data: 01/2010 to 12/2019

	period	spacing	repeat	#obs
C-2	01/11-12/19	8 km	369 d	1.87 M
J-1	01/10-03/12	315 km	10 d	0.52 M
J-1 GM	05/12-06/13	7.5 km	406 d	0.27 M
J-2	01/10-05/17	315 km	10 d	1.79 M
J-2 GM	07/17-09/17	8.5 km	371 d	0.04 M
J-3	02/16-12/19	315 km	10 d	0.95 M

as processed and distributed by AVISO [12]

Configuration of Numerical Experiment

Study region

200 km mesh created by JIGSAW [6]

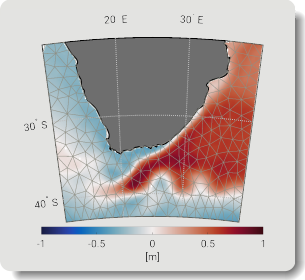

Gravity field information

- satellite-only model
- unconstrained GOCO06S normal equations
- spherical harmonic degree 2 to 300
- further details: [7]

Along track SSH data: 01/2010 to 12/2019

	period	spacing	repeat	#obs
C-2	01/11-12/19	8 km	369 d	1.87 M
J-1	01/10-03/12	315 km	10 d	0.52 M
J-1 GM	05/12-06/13	7.5 km	406 d	0.27 M
J-2	01/10-05/17	315 km	10 d	1.79 M
J-2 GM	07/17-09/17	8.5 km	371 d	0.04 M
J-3	02/16-12/19	315 km	10 d	0.95 M

as processed and distributed by AVISO [12]

Estimated parameters

- SH to degree 600: 361 197 parameters
- FE MDT: 1195
- FE OV: 3×1195 (model B)
- 3 intermission biases

Regularization/smoothness

- SH: Kaula degree 201 until 600, empirical weight
- FE MDT: min $\|\nabla\zeta(\theta,\lambda)\|$, empirical weight
- FE OV: $\|\nabla OV(\theta,\lambda,t)\|$ (scen B), weight by VCE

Assembly and solution full least-squares normal equations

- Model A (static): 490 GB
- Model B (temporal): 506 GB

⇒ implementation in HPC environment

Model A – CNES_CLS18

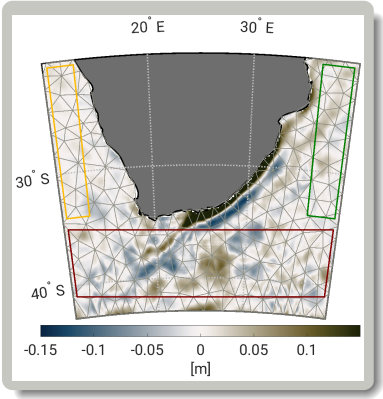

RMS Region 1: 0.9 cm
RMS Region 2: 1.6 cm
RMS Region 3: 3.6 cm
RMS: 5.1 cm

MDT Solutions Compared to CNES_CLS18

Model A – CNES_CLS18

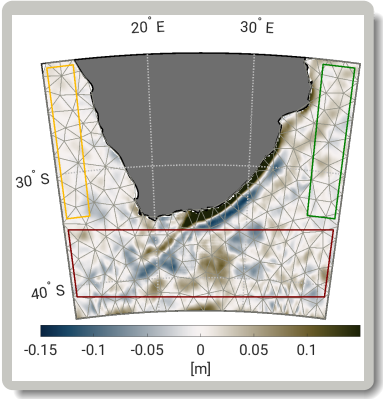

RMS Region 1: 0.9 cm
RMS Region 2: 1.6 cm
RMS Region 3: 3.6 cm
RMS: 5.1 cm

Model B – CNES_CLS18

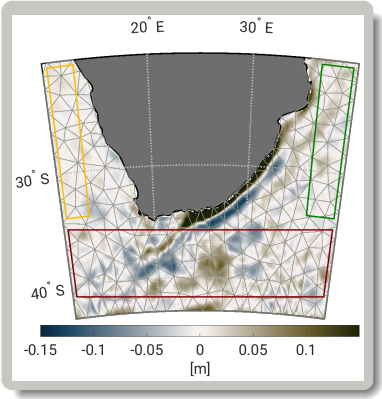

RMS Region 1: 0.9 cm
RMS Region 2: 1.6 cm
RMS Region 3: 3.7 cm
RMS: 5.1 cm

MDT Solutions Compared to CNES_CLS18

Model A – CNES_CLS18

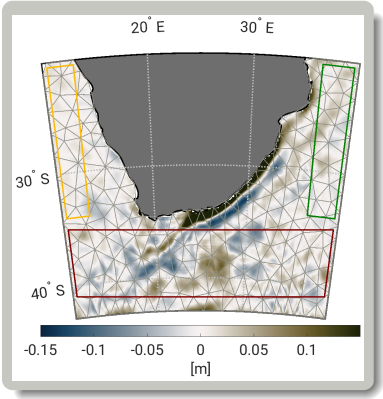

RMS Region 1: 0.9 cm
RMS Region 2: 1.6 cm
RMS Region 3: 3.6 cm
RMS: 5.1 cm

Model B – CNES_CLS18

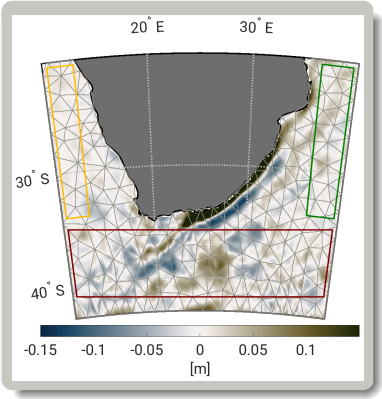

RMS Region 1: 0.9 cm
RMS Region 2: 1.6 cm
RMS Region 3: 3.7 cm
RMS: 5.1 cm

Model B – Model A

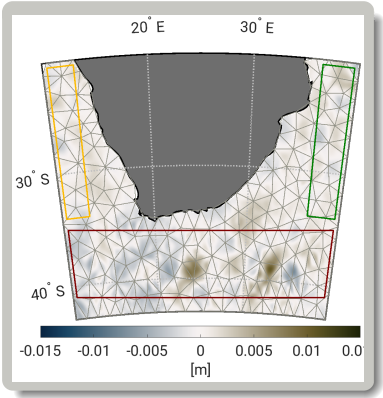

RMS Region 1: 0.1 cm
RMS Region 2: 0.1 cm
RMS Region 3: 0.2 cm
RMS: 0.2 cm

Geoid Solutions Compared to XGM2019 at d/o 760

Model A – XGM2019

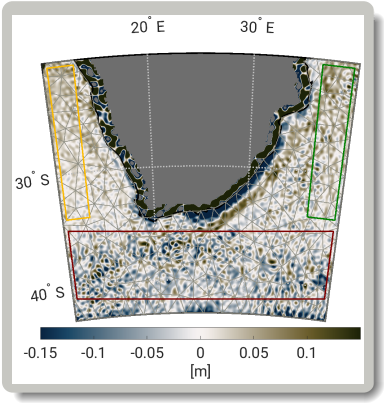

RMS Region 1: 2.0 cm
RMS Region 2: 3.5 cm
RMS Region 3: 5.3 cm
RMS: 10.0 cm

Geoid Solutions Compared to XGM2019 at d/o 760

Model A – XGM2019

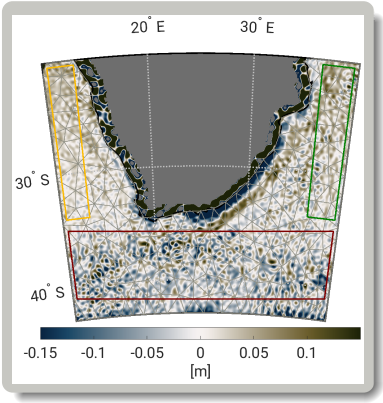

RMS Region 1: 2.0 cm
RMS Region 2: 3.5 cm
RMS Region 3: 5.3 cm
RMS: 10.0 cm

Model B – XGM2019

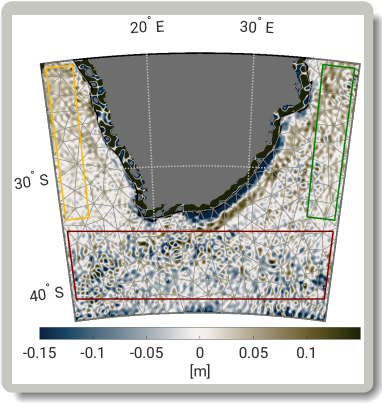

RMS Region 1: 2.0 cm
RMS Region 2: 3.5 cm
RMS Region 3: 5.3 cm
RMS: 10.0 cm

Geoid Solutions Compared to XGM2019 at d/o 760

Model A – XGM2019

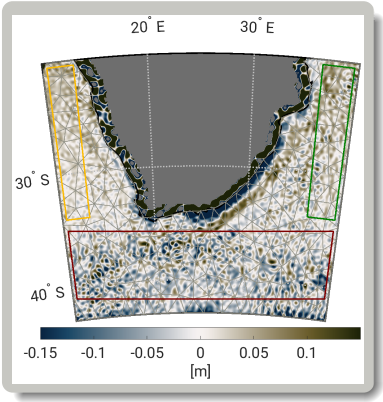

RMS Region 1: 2.0 cm
RMS Region 2: 3.5 cm
RMS Region 3: 5.3 cm
RMS: 10.0 cm

Model B – XGM2019

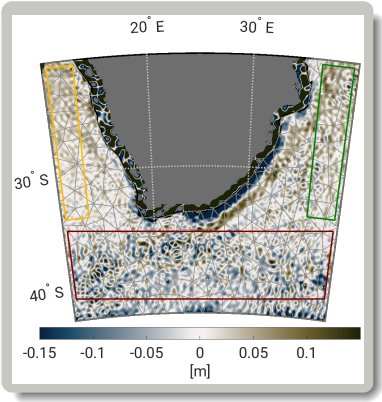

RMS Region 1: 2.0 cm
RMS Region 2: 3.5 cm
RMS Region 3: 5.3 cm
RMS: 10.0 cm

Model B – Model A

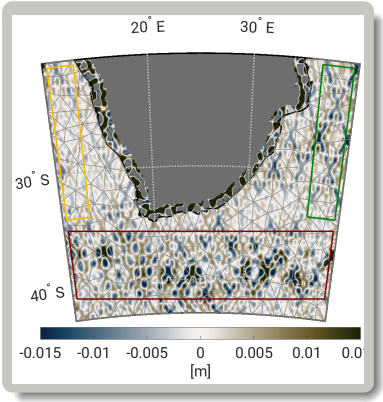

RMS Region 1: 0.3 cm
RMS Region 2: 0.5 cm
RMS Region 3: 0.7 cm
RMS: 0.8 cm

Validating Estimated Ocean Variability

Coestimated in Model B

From gridded DUACS daily SLA maps [13]

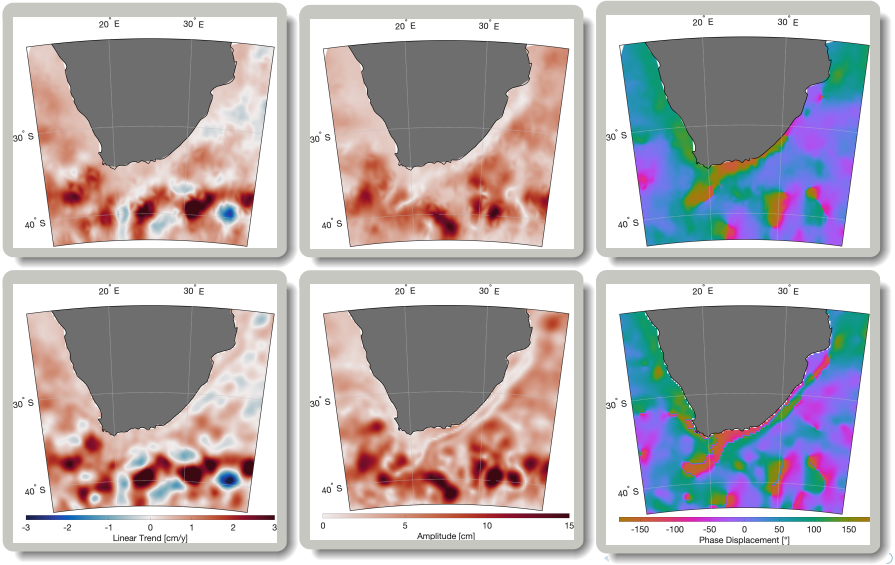

Summary and Conclusions

- coestimation of long-term temporal signal possible
- reasonable signal in areas of lower ocean variability
- but temporal model (trend and seasonal period) for regions of higher variability insufficient

OV as time series

Point in region of low variability

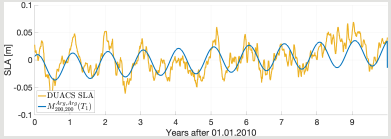

Point in region of high variability

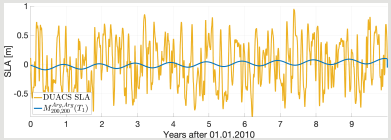

Summary and Conclusions

- coestimation of long-term temporal signal possible
- reasonable signal in areas of lower ocean variability
- but temporal model (trend and seasonal period) for regions of higher variability insufficient

- no obvious gain for MDT estimation (5 mm)
- no obvious gain for geoid estimation (10 mm)

⇒ FE & adjustment serves as spatio-temporal filter (200 km)

OV as time series

Point in region of low variability

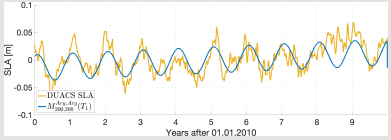

Point in region of high variability

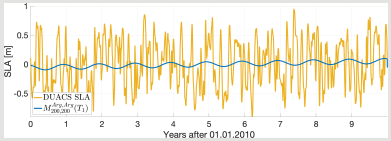

Summary and Conclusions

- coestimation of long-term temporal signal possible
- reasonable signal in areas of lower ocean variability
- but temporal model (trend and seasonal period) for regions of higher variability insufficient

- no obvious gain for MDT estimation (5 mm)
- no obvious gain for geoid estimation (10 mm)

⇒ FE & adjustment serves as spatio-temporal filter (200 km)

- weighting of smoothness/regularization
- influence on regional intermission bias estimation (up to 2 cm between models A and B)
- improve the temporal modeling (cf. Borlinghaus et al.)?
- improve the separation in general (drifter, RSV,...)

OV as time series

Point in region of low variability

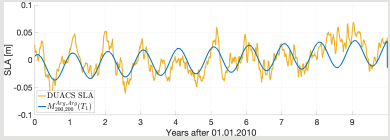

Point in region of high variability

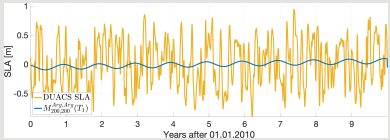

References I

[1] J. H. Argyris, I. Fried, and D. W. Scharpf. The TUBA Family of Plate Elements for the Matrix Displacement Method. *The Aeronautical Journal*, 72(692):701–709, August 1968. ISSN 0001-9240, 2059-6464. doi: 10.1017/S000192400008489X. URL https://www.cambridge.org/core/journals/aeronautical-journal/article/tuba-family-of-plate-elements-for-the-matrix-displacement-method/2E7280F506997FC8A8357C30B5334D9D.

[2] S. Becker, J. M. Brockmann, and W.-D. Schuh. Mean dynamic topography estimates purely based on GOCE gravity field models and altimetry. *Geophysical Research Letters*, 41(6):2063–2069, March 2014. ISSN 1944-8007. doi: 10.1002/2014GL059510. URL http://onlinelibrary.wiley.com/doi/10.1002/2014GL059510/abstract.

[3] S. Becker, M. Losch, J. M. Brockmann, G. Freiwald, and W.-D. Schuh. A Tailored Computation of the Mean Dynamic Topography for a Consistent Integration into Ocean Circulation Models. *Surveys in Geophysics*, 35 (6):1507–1525, November 2014. ISSN 0169-3298, 1573-0956. doi: 10.1007/s10712-013-9272-9. URL http://link.springer.com/article/10.1007/s10712-013-9272-9.

[4] J.M. Brockmann, C. Neyers, and W.-D. Schuh. A Parametric Representation to Integrate Current Observations into the Estimation of the Mean Dynamic Topography (poster). Poster, 2019.

References II

[5] R.W. Clough and J.L. Toche. Finite Element Stiffness Matrices for Analysis of Plate Bending. Technical Report AFFDL-TR-66-80, Air Force Flight Dynamics Laboratory; University of California, Berkeley, 1966. URL `http://contrails.iit.edu/reports/8574`.

[6] Darren Engwirda. JIGSAW-GEO (1.0): Locally orthogonal staggered unstructured grid generation for general circulation modelling on the sphere. *Geoscientific Model Development*, 10(6):2117–2140, June 2017. ISSN 1991-959X. doi: 10.5194/gmd-10-2117-2017. URL `https://www.geosci-model-dev.net/10/2117/2017/`.

[7] Andreas Kvas, Jan Martin Brockmann, Sandro Krauss, Till Schubert, Thomas Gruber, Ulrich Meyer, Torsten Mayer-Gürr, Wolf-Dieter Schuh, Adrian Jäggi, and Roland Pail. GOCO06s – a satellite-only global gravity field model. *Earth System Science Data*, 13(1):99–118, January 2021. ISSN 1866-3508. doi: 10.5194/essd-13-99-2021. URL `https://essd.copernicus.org/articles/13/99/2021/`.

[8] Silvia Müller, Jan Martin Brockmann, and Wolf-Dieter Schuh. Consistent Combination of Gravity Field, Altimetry and Hydrographic Data. In Urs Marti, editor, *Gravity, Geoid and Height Systems*, number 141 in International Association of Geodesy Symposia, pages 267–273. Springer International Publishing, 2014. ISBN 978-3-319-10836-0 978-3-319-10837-7. doi: 10.1007/978-3-319-10837-7_34. URL `http://link.springer.com/chapter/10.1007/978-3-319-10837-7_34`.

[9] C. Neyers. *Integration von Radialen SAR Doppler Ozeanoberflächengeschwindigkeitsmessungen in Die Berechnung Der Dynamischen Ozeantopographie*. M.Sc. Thesis, Universität Bonn, Bonn, Germany, 2017.

References III

[10] Christian Neyers, Jan Martin Brockmann, and Wolf-Dieter Schuh. Parametric finite element based models to represent the Mean Dynamic Ocean Topography, 2019.

[11] Roland Pail, Alberta Albertella, Daniel Rieser, Jan Martin Brockmann, Wolf-Dieter Schuh, and Roman Savcenko. Satellite Gravity Models and Their Use for Estimating Mean Ocean Circulation. In Chris Rizos and Pascal Willis, editors, *Earth on the Edge: Science for a Sustainable Planet*, number 139 in International Association of Geodesy Symposia, pages 275–281. Springer Berlin Heidelberg, 2014. ISBN 978-3-642-37221-6 978-3-642-37222-3. doi: 10.1007/978-3-642-37222-3_36. URL `http://link.springer.com/chapter/10.1007/978-3-642-37222-3_36`.

[12] Laurent Soudarin, Françoise Mertz, Vinca Rosmorduc, Catherine Schgounn, Thierry Guinle, Florence Birol, and Fernando Niño. Aviso+: What's new on the reference portal in satellite altimetry? *EGU General Assembly Conference Abstracts*, 16:19669, 2014. doi: 10.5194/egusphere-egu2020-19669. URL `https://ui.adsabs.harvard.edu/abs/2020EGUGA..2219669S`.

[13] Guillaume Taburet, Antonio Sanchez-Roman, Maxime Ballarotta, Marie-Isabelle Pujol, Jean-François Legeais, Florent Fournier, Yannice Faugere, and Gerald Dibarboure. DUACS DT2018: 25 years of reprocessed sea level altimetry products. *Ocean Science*, 15(5):1207–1224, September 2019. ISSN 1812-0784. doi: 10.5194/os-15-1207-2019. URL `https://os.copernicus.org/articles/15/1207/2019/`.